Desalination and Water Treatment
www.deswater.com

doi: 10.1080/19443994.2015.1048532

57 (2016) 11859–11871
May

Taylor & Francis
Taylor & Francis Group

Biogenic synthesis of magnetic perlite@iron oxide composite: application as a green support for dye removal

Mahsa Shirkhodaie, Mostafa Hossein Beyki, Farzaneh Shemirani*

School of Chemistry, University College of Science, University of Tehran, P.O. Box 14155-6455, Tehran, Iran,
Tel. +98 21 61112481; emails: M.shirkhodaie@gmail.com (M. Shirkhodaie), Hosseinbakim@gmail.com (M. Hossein Beyki),
Tel. +98 21 61112481; Fax: +98 21 66405141; emails: Shemiran@khayam.ut.ac.ir, Shemiran_farzaneh@yahoo.com (F. Shemirani)

Received 19 August 2014; Accepted 21 April 2015

ABSTRACT

This study presents a method to synthesize magnetic expanded perlite composite through a co-precipitation method using single iron source and yellow pea as a reducing agent. The suggested method is environment friendly, easy, and biogenic. The combination of magnetite nanoparticles with expanded perlite and its modification with ibuprofen resulted in a new, cost-effective, and eco-friendly magnetic adsorbent for dye removal from contaminated streams. The prepared composite was characterized by point of zero charge (pH_{zpc}), X-ray diffraction, scanning electron microscopy, vibration sample magnetometer, and Fourier transforms infrared spectroscopy (FT-IR). The prepared adsorbent was used to remove Direct Red-81 as a target pollutant to test the feasibility of this idea, UV–vis spectroscopy was used to follow the adsorption process. The maximum adsorption was observed within 1 min at pH 4–6 using 30 mg of adsorbent. The experimental data were analyzed by the Langmuir and Freundlich adsorption models. Both models provided the best correlation of the experimental data and the maximum capacity was found to be 416.66 mg g^{-1} under the optimized conditions. Desorption process of the anionic dye adsorbate was also investigated using ethanol as an eluent, and the volume of eluent was optimized.

Keywords: Dye removal; Green chemistry; Ibuprofen; Magnetic composite; Perlite

1. Introduction

In view of the global concern over the problems associated with environmental contaminants, the utilization of remediation techniques—especially those in which nontoxic chemicals, and renewable materials are used—has gained quite a bit of interest [1–6]. Among various environmental remediation technologies such as filtration [7], ion exchange [8], adsorption [9,10], chemical precipitation [11], and electrochemical oxidation [12], adsorption has gained more attention recently owing to its simple design, ease of operation and handling, low-cost, as well as the capability of being a green process [13,14]. It is worth noting that the type of adsorbent plays an important role in the effectiveness of this process [15]. With this in mind, over the last few years, several attempts have been made to develop natural, low-cost materials with a good retention capacity as adsorbents in order to make the adsorption method less expensive, more effective, and a green technique. Among the reported low-cost adsorbents, mineral materials, such as clay,

*Corresponding author.

1944-3994/1944-3986 © 2015 Balaban Desalination Publications. All rights reserved.

zeolites, and siliceous minerals, have been preferentially applied in adsorption studies because of their good mechanical and chemical stability as well as their resistance to microbiological degradation, [14,16–19]. Perlite (PT), a naturally occurring glassy volcanic siliceous rock with both unique physical and chemical properties, is one of these mineral compounds, which has attracted a great deal of attention in different areas, especially when it is heated rapidly at 760–1,100˚C. By being heated, it expands up to 20 times of its original volume and forms a light white mineral. It is chemically inert and nontoxic, and furthermore there are different types of silanol groups and alumina's hydrous oxide on its surface. Consequently, it can be classified as a natural, low-cost adsorbent for the removal of heavy metals and organic contaminants [20–23]. There are several reports in the literature on the application of expanded PT as an adsorbent for the removal of such dyes as Victoria blue [24], Methyl violet [25], Congo red [26], and Methylene blue [27]. In all these reports, dyes are adsorbed on nonmodified expanded PT, while, by modifying it chemically, the interactions between an adsorbent and dyes can be enhanced. It is worth noting that the adsorption technique as a removal method would be problematic, inasmuch as it is difficult and time-consuming to recover the conventional adsorbents and separate them from the solution whether by high-speed centrifugation or by filters [28]. Researchers have shown much interest in overcoming this limitation through the use of magnetic and magnetizable adsorbents rather than nonmagnetic ones, by means of which separation could be done magnetically by applying an appropriate magnetic field [29,30]. A variety of methods have been reported in the literature to synthesize magnetite nanoparticles, among which chemical precipitation, using only one iron source and appropriate reducing agent, is attracting increasing interest owing to its being cost-effective [31]. Nonetheless, using reagent grade chemicals as solvents and reducing agents—which are expensive, toxic, and environmentally unfriendly—in the synthesis of magnetic nanoparticles (MNPs) often limit its large-scale applications. [32]. Thus, the green synthesis of such nanoparticles, using naturally occurring reagents, not only can reduce the costs and the toxicity of the resulting materials, but also can diminish the environmental impacts of the byproducts [33–37]. However, just a limited number of studies have been reported, where natural materials rather than chemicals have been used in the synthesis of Fe_3O_4 nanoparticles in which soybean sprout [38], glucose [32], maltose [39], brown seaweed [40], and various reducing sugars were employed as natural reducing reagent [34].

There are few studies conducted on the adsorption of dyes by a modified magnetic expanded PT. Magnetic expanded perlite (MPT) has hydroxyl, Si–O–Si, and Fe–O groups. According to the literature, the adsorption of anionic dyes on the expanded perlite has occurred at a specific pH due to electrostatic interactions [41]. For improving the adsorption of dyes, an organic agent consisting aromatic rings could be a good choice for the modification of the MPT. In this study, for the first time, a green approach to synthesize Fe_3O_4 nanoparticles, using yellow pea powder as a reductant, was employed. Ibuprofen was selected as an organic agent in the modification process in that it is nontoxic and cost-effective. Bonding ibuprofen to the MPT was done through a refluxing rout, which yielded a product with an ester group. The synthesized composite was used as a novel adsorbent for anionic dye removal. According to our knowledge, there are few reports either on preparing magnetic perlite, using biogenic route, or on chemically modifying MPT with nontoxic organic agent such as ibuprofen. Direct Red-81 (DR-81) was selected for this study as a test sample. The effects of various parameters such as pH, contact time, adsorbent dosage, and initial dye concentration were also investigated on its removal.

2. Experimental section

2.1. Materials and instrumentation

The DR-81 which was used as a model dye was supplied from chemistry & chemical engineering research center of Iran. It is widely used in several industries, and also it is azo-based. Thus, its elimination from effluent is important [42]. The stock dye solution was prepared by dissolving an appropriate amount of dye powder in distilled water. The pH was adjusted using HCl or NH_3. Toluene, acetone, $Fe(NO_3)_3.9H_2O$ (Merck, Darmstadt, Germany), ground yellow pea, and ibuprofen (prepared by Arya pharmaceutical company, Tehran, Iran) were used to synthesize adsorbent. Expanded perlite was obtained from Kaneh Azar Co. (Tabriz, Iran). The pH-Meter model 781 from Metrohm (Herisau, Switzerland) equipped with glass combination electrode was used for the pH measurements. The adsorption studies of the test solutions were carried out using a UV–vis spectrophotometer model Perkin Elmer (Lambda 25). The FT-IR study of the samples was done by Equinox 55 Bruker with ATR method over the wavelength of 400–4,000 cm^{-1}. The scanning electron microscopy (SEM) (model KYKY-3200. Beijing, China) was used to investigate morphology of the composite. X-ray

diffraction (XRD) measurements were performed using a STADI-MP from a STONE company (Germany) with monochromatized Cu Kα radiation. Magnetization investigation was done using a vibration sample magnetometer (VSM) (Lake Shore Model 7400, Japan). Strong Magnet with 1.31 magnet field was used for magnetic separation.

2.2. Preparation of perlite@Fe_3O_4 composite

Magnetic expanded PT composite was synthesized via an ultrasound assisted co-precipitation method using only one iron source and natural reducing agent. In a typical experimental procedure, 1.5 g of $Fe(NO_3)_3.9H_2O$ was added into 10 ml of solution containing 0.2 g of ground yellow pea. The mixture was stirred for 1 h at 60˚C. Then, while maintaining stirring, 2.5 g of expanded PT was added to the mixture. After 30 min of stirring, 1 ml of NH_3 (25%) was added dropwise into the mixture under ultrasound radiation. By doing so, the color of resultant mixture turned into black which indicated the formation of magnetic Fe_3O_4. The resulting mixture was heated at 80˚C for about 1 h in ultrasound clean bath. Later, it was cooled to a room temperature and obtained black product was isolated by applying an external magnetic field, washed with distilled water. Afterward, dried in the oven at 80º for 4 h and stored for further use.

2.3. Modification of magnetic composition

Magnetic expanded PT was modified by the simple method. To do so, initially, 0.5 g of Ibuprofen was dissolved in 20 ml of Toluene. The mixture was added to the 1.0 g of magnetic perlite composite which was in the boiling flask, then about 0.1 ml of sulfuric acid was added to it, and afterward, the mixture was heated to reflux while stirring for 12 h. The obtained product was separated by a magnet and washed several times with ethanol, and then dried at the room temperature. The preparation of composite is illustrated in Fig. 1.

2.4. Point of zero charge (pHzpc)

The pH_{zpc} of samples was determined by the batch equilibration technique [23,24]. In order to do so, 10 mg of the MPT was added to 20 ml of NaCl solution (5.8×10^4 mg · L^{-1}). The initial pH value (pH_i) of NaCl solution was adjusted from 1 to 7 by addition of 3.6×10^4 mg · L^{-1} of HCl and 1.7×10^4 mg · L^{-1} NH_3. The suspension reached equilibration at 25˚C by stirring for 24 h. Finally, it was collected with external magnetic field. The final pH value (pH_f) was measured. The pH_{zpc} was obtained from the plot of pH_f versus pH_i value. (Fig. 4(b)).

2.5. Adsorption procedure

Experiments were performed using batch equilibrium technique. To do so, about 30 mg of modified composite was added to 50 ml of DR-81 solution of known concentration. After adjustment of pH to 6.0, it was shaken for 1 min to reach the equilibrium. At the end of adsorption period, by applying magnetic field the dye solution was separated from adsorbent. Then, concentration of residual analyte was determined by measuring the absorbance at 509.73 nm using a UV–vis spectrophotometer.

The amount of dye adsorbed at equilibrium onto magnetic nanocomposite, Q_e $(mg\,g^{-1})$, was calculated by following equation:

$$Q_e = (C_i - C_e)V/m \quad (1)$$

where C_i and C_e $(mg \cdot L^{-1})$ are initial and equilibrium liquid phase concentrations of DR-81, respectively. V is the volume of the solution (L), and m is the weight (g) of the modified magnetic perlite composite.

3. Results and discussion

3.1. Adsorbent characterization

The SEM analysis gives a sufficient general overview of the surface morphology and fundamental physical properties of the adsorbent. Fig. 2 shows SEM images of expanded PT and modified magnetic expanded PT. The SEM image of the expanded PT (Fig. 2(a)) shows the glassy structure and irregular plates with broken edge; open pores, as well as small channels that form a thick network. These particles are 5–100 μm in length and about 80 nm in thickness. As it is illustrated in Fig. 2(b) and (c), the modified magnetic expanded PT, shows better dispersity in comparison to expanded perlite. Moreover, the particle size is less than 100 nm.

Fig. 2(d) shows XRD patterns of expanded PT and magnetic expanded PT. It indicates that the nature of silica in expanded PT is mainly amorphous with irregular morphology. Comparison between XRD pattern of expanded PT and magnetic composite shows the effect of its magnetization. It is found that all the reflection peaks at (1 1 1), (2 2 0), (3 1 1), (4 0 0), (4 2 2), (5 1 1), (4 4 0) can be well indexed to the inverse cubic spinel structure of Fe_3O_4 (JCPDS card

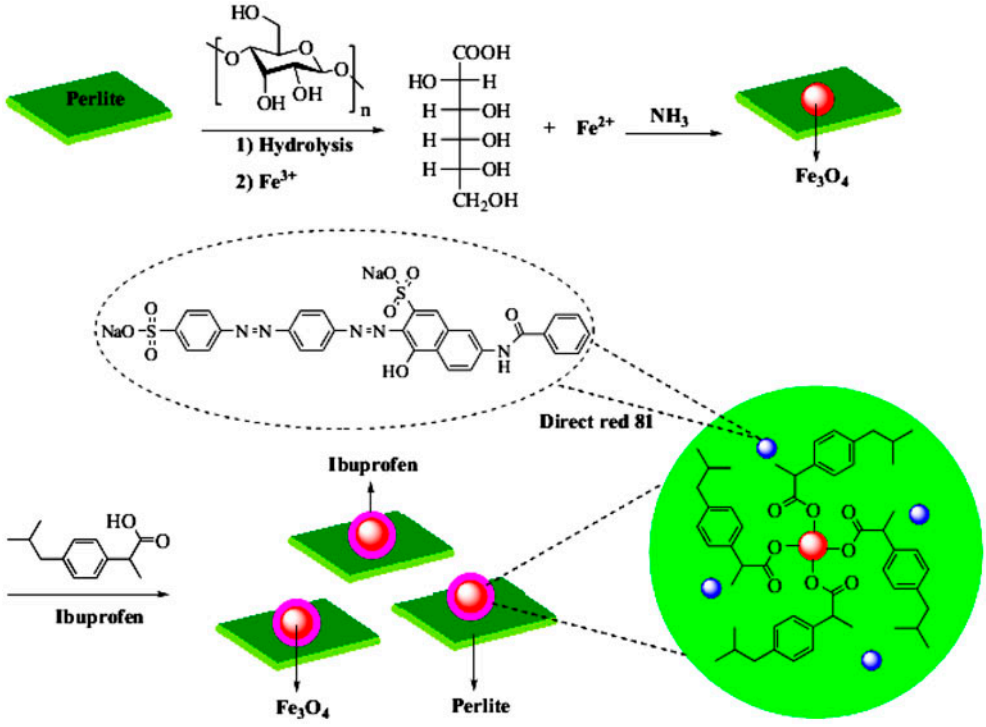

Fig. 1. General procedure for preparation of MPT and ibuprofen modified composite.

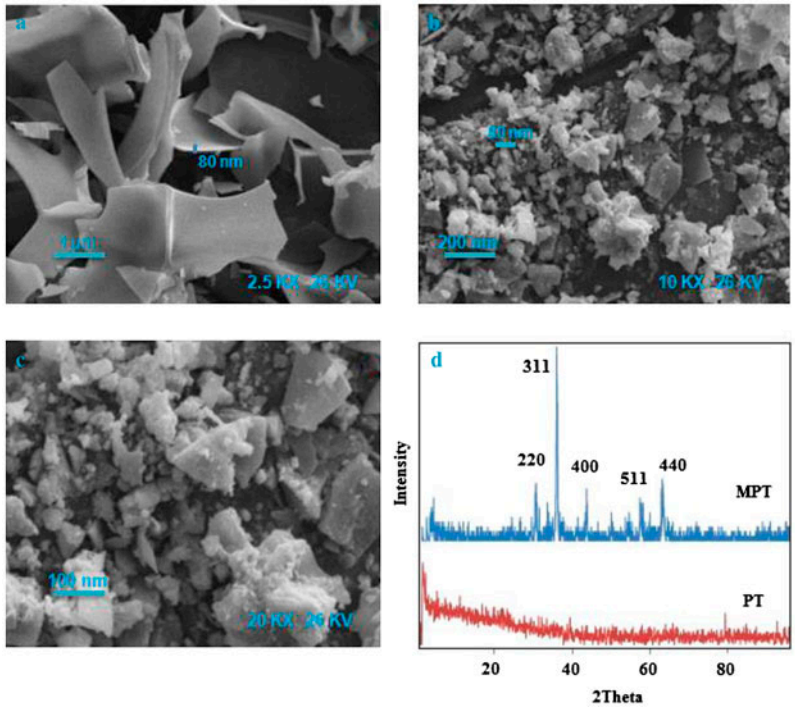

Fig. 2. SEM images of expanded perlite (a) and MPT (b, c), XRD patterns of perlite (PT) and MPT (d).

No. 75-1610) according to the reflection peak position and relative intensities, which confirms that the nanoparticle synthesized in this study are the Fe_3O_4.

Fig. 3(a) shows the FT-IR spectra of magnetic composite and modified magnetic material in the spectrum of magnetic expanded PT, the broad peaks around 3,000 cm^{-1} is indicative of existence of bonded hydroxyl groups and the band at 1,022 cm^{-1} is assigned to the Si–O–Si. Characteristic bands from Fe–O stretching vibrations are observed at 466–565 cm^{-1}. Also a spectrum of the modified sorbent is dominated by the bands of the magnetic expanded PT. In addition, the presence of surfactant is also observable. In this regard, the appearance of new band at 1,665 cm^{-1} can be attributed to the C=O group. Additionally, the broad band at 2,800 can be attributed to −CH vibration. The C–O antisymmetric stretching and C–O–C vibration at 1,164 and 1,111 cm^{-1} are not observable owing to the overlapping with silicate bands.

The magnetic property of the prepared composite was carried out using a VSM at room temperature. Fig. 3(b) reveals that the value of saturation magnetization is 14.73. In addition, remnant magnetization and coercivity are 38.51 and 0.49, respectively, which are negligible and indicating that the prepared magnetic composite has superparamagnetic characteristic.

3.2. Effect of pH

The pH of the dye solution plays an important role on the adsorption capacity, in that it affects both aqueous charge distribution and the surface binding site of the sorbent. In this study, the influence of pH on adsorption capacity of DR-81 onto modified magnetic composite in the range of pH values from 1 to 10 at a fixed dye concentration of 20 $mg \cdot L^{-1}$ and also fixed adsorbent optimum dosage of 0.03 g, was investigated. As it was indicated in results (Fig. 4(a)), adsorption capacity decreased with an increase in pH from 6 to 8 then slowly decreased as pH rose from 8 to 9. The adsorption mechanism includes not only the π–π interactions but also electrostatic attractive force between analyte and ibuprofen modified MPT. The share of electrostatic interaction is higher, however. This could be explained on the basis of zero point charge adsorption (pH_{ZPC}), which is six in this study (Fig. 4(b)). The adsorbent surface was more positively charged when the dye solution pH was lower than pH_{ZPC}. In other words, it was negatively charged at the pH greater than pH_{ZPC}. With this in mind, at pH values above six, the negatively charged adsorbent surface repelled the anionic dyes (DR-81). Thus, the adsorption capacity decreases. The adsorption of anions was favored at $pH < pH_{ZPC}$ owing to the development of positive charge at the surface of the adsorbent. The maximum adsorption occurred at pH 4–6 which is counterbalanced by anionic dye and implies that this sorbent is a very promising one for anionic dye removal in a wide pH range.

3.3. Effect of pH on the azo dyes absorbance properties

Many azo dyes are pH-dependent; absorbance of them may vary because of the pH variation. It is generally due to a change in the charge on the dye molecules or a change in the level of conjugation. In order to investigate the effect of pH on the DR-81 dye's absorbance properties, the pH of the direct red solutions (20 mg L^{-1}) were adjusted to several pH and their absorbance properties were determined using a UV–vis spectrophotometer. As it can be shown form Fig. 5(a), the maximum absorbance length of direct red was not changed by changing pH.

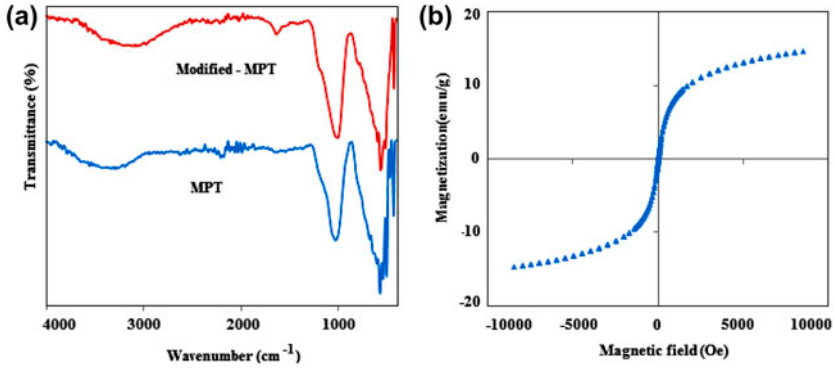

Fig. 3. FT-IR spectra of magnetic perlite and modified MPT (a), VSM graph of MPT (b).

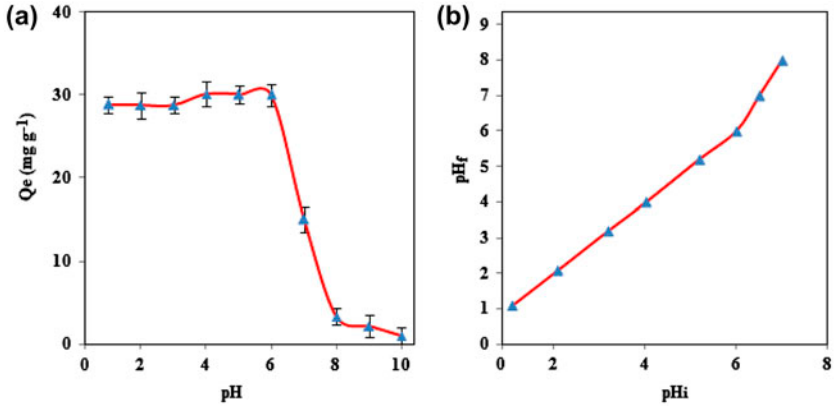

Fig. 4. Effect of pH on equilibrium adsorption capacity of DR-81 onto modified magnetic perlite (dye concentration (C_0) = 20 mg L^{-1}, adsorbent dosage: 30 mg; contact time: 1 min) (a), zero point charge (pH_{ZPC}) of the modified MPT (b).

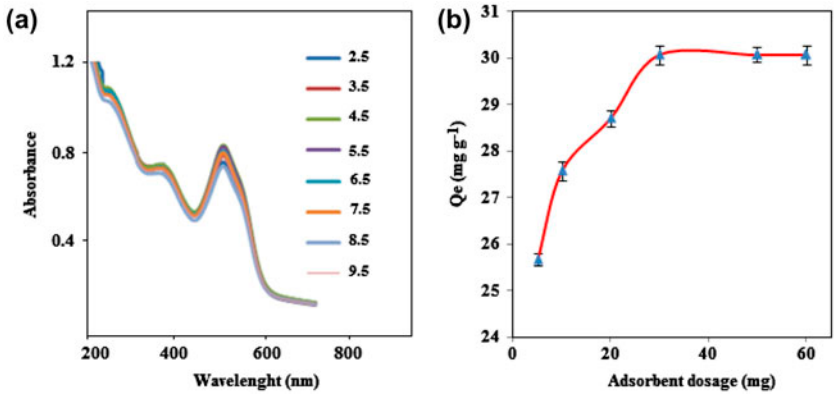

Fig. 5. Effect of pH on DR-81 absorbance properties (a) effect of adsorbent dosage on equilibrium adsorption capacity of DR-81 onto modified MPT (b).

3.4. Effect of adsorbent dosage

The effect of adsorbent dosage on the removal of DR-81 was studied by changing the dosage of modified adsorbent, which ranged from 0.01 to 0.06 g by keeping constant initial dye concentration (20 mg · L^{-1}) of 50 ml of dye solution at optimum pH (4–6) and equilibrium time (1 min). As it could be seen in Fig. 5(b) rapid increase in the adsorption upon increasing adsorbent dosage is owing to higher number of adsorption site. A further increase in adsorbent dosage from 0.03 to 0.06 g made a slight increase in the dye removal hence, 0.03 g was selected as optimum amount of sorbent for dye removal.

3.5. Adsorption isotherms

In order to both understand the capacity of adsorbent and evaluate its adsorption properties it is important to investigate adsorption isotherms which could be helpful in designing of adsorption system, and also could illustrate how adsorbate interacts with adsorbent under the optimum condition. In this study, adsorption isotherms data were analyzed according to the Langmuir and Freundlich models. The Langmuir model is based on the assumption that adsorption occurs at specific homogeneous monolayer surface containing sites with uniform energy, and there is no interaction between adsorbate molecules. After completion of adsorbed monolayer, saturation of active sites occurs. Therefore, the adsorption of adsorbate stops, and no more interaction takes place between the adsorbent and adsorbate molecules [14,32,43].

The linear Langmuir isotherm equation can be written as followed:

$$C_e/Q_e = C_e/Q_m + \frac{1}{Q_m K_a} \quad (2)$$

where C_e is the equilibrium concentration (mg·L^{-1}), Q_e is the amount adsorbed by the dye at equilibrium (mg g^{-1}), Q_m is the maximum adsorption capacity of a monolayer (mg g^{-1}) and K_a is the energy of adsorption (Langmuir constant, L mg^{-1}). The values of Q_m and K_a were calculated from the slope and intercept of plot of C_e/Q_e versus C_e (Fig. 6(a) and (c)). The value of the dimensionless parameter R_L which is the measure of adsorption favorability is calculated according to Eq. (3):

$$R_L = 1/(1 + C_0 K_a) \quad (3)$$

The R_L value was found in the range of $0 < R_L < 1$ which indicated a favorable adsorption process.

Freundlich isotherm describes that adsorption occurs on a heterogeneous surface, and hence does not assume monolayer capacity. The adsorption occurs at sites with different energies and the energy of adsorption varies as a function of surface coverage [44]. The linear form of Freundlich isotherm is expressed as:

$$\log Q_e = \log K_f + 1/n \log C_e \quad (4)$$

K_f and n are calculated from the intercept and slope of the linear plot of log Q_e vs. log C_e (Figs. 6(b) and (d)).

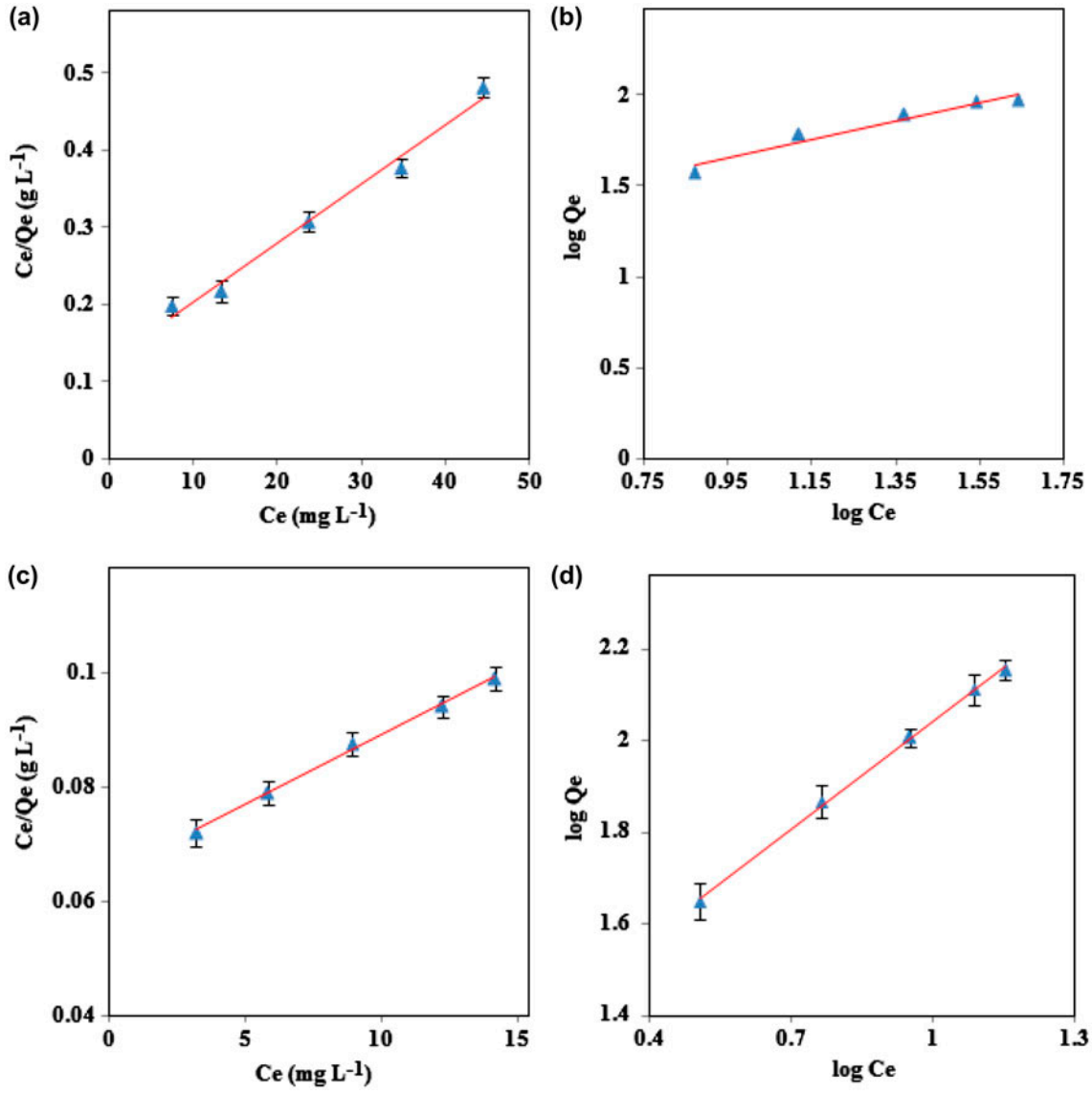

Fig. 6. Langmuir and Freundlich adsorption isotherm of DR-81 onto nonmodified (a, b) and modified magnetic perlite (c, d).

The values of Langmuir and Freundlich constants; as well as the correlation coefficients (R^2) for both modified and nonmodified composite are summarized in Table 1. As it can be seen, experimental data fit with both models as values of the correlation coefficient (R^2) are close to one. The applicability of these two isotherms to the dyes adsorption shows that both monolayer adsorption and heterogeneous energetic distribution of active sites on the surface of the adsorbent are possible. However, to determine the best-fitting model, nonlinear chi-squared (χ^2) test have been used to evaluate isotherm model fitness. The χ^2 can be defined mathematically as:

$$\chi^2 = \sum \left[\left(Q_{e,exp} - Q_{e,cal} \right)^2 / Q_{e,cal} \right] \quad (5)$$

where $Q_{e,exp}$ and $Q_{e,cal}$ are the experimental data and calculated from nonlinear models [45]. According to the results (Table 1 and Fig. 7(a) and (b)), the Langmuir isotherm model shows better fitness. Moreover, it was observed that the Langmuir equation give a lower values of the chi-squared test compared to Freundlich isotherm and suggests that the Langmuir model is the better model describing sorption behavior.

Maximum adsorption capacity for nonmodified adsorbent is 142.8 mg g^{-1} that increased to 416.66 for modified composite. This reveals that the modification process increased the efficiency of magnetic perlite for dye removal.

Table 2 compares the adsorption capacity of ibuprofen modified MPT with different types of adsorbents previously used for removal of anionic dyes. It can be seen that adsorption capacity of anionic dyes on this modified expanded perlite is much higher than that of many other previously reported adsorbents.

Table 1
Langmuir and Freundlich parameters for the adsorption of the DR-81 onto modified and nonmodified magnetic perlite

Isotherm		Nonmodified	Modified
	R_L	0.15–0.37	0.21–0.57
	R^2	0.98	0.99
Langmuir	K_a	0.05	0.03
	Q_m	142.85	416.66
	χ^2	0.34	0.36
	R^2	0.95	0.99
Freundlich	N	1.94	1.27
	K_f	14.12	18.10
	χ^2	2.07	1.22

Moreover, the adsorption process on this adsorbent is much faster than the adsorption onto other adsorbent. This indicates that the modified expanded perlite can be considered as a promising adsorbent for the removal of anionic dyes from aqueous solutions.

3.6. Kinetic models

Among several kinetic models, five of the main models were applied to the experimental data to determine the kinetic parameters and investigate the mechanism of adsorption of DR-81\by magnetic Fe_3C_4@perlite as an adsorbent. Kinetic measurements were made under the optimum conditions by batch extraction at different times. The results are summarized in Table 3. The rate of the adsorptive interactions can be evaluated using the linear form of integrating the Lagergren pseudo-first-order equation, which is the most widely used procedures for the adsorption of solute from aqueous solution. The boundary condition $t = 0$ to $t = t$ and $Q_t = 0$ to $Q_t = Q_t$.

$$\ln\left(Q_e - Q_t\right) = \ln Q_t - k_1 t \quad (6)$$

where k_1 is the pseudo-first-order adsorption rate constant and Q_e, Q_t are the values of the amount adsorbed per unit mass at equilibrium and at any time t $\left(\text{mg g}^{-1}\right)$. The values of Q_e and k_1 $\left(\text{mg g}^{-1}\,\text{min}^{-1}\right)$ can be determined experimentally by plotting, $\ln(Q_e - Q_t)$ versus t, as it is shown obtained plot (Fig. 8(a)) is linear ($R^2 = 0.97$) and also there is an acceptable difference between the experimental Q_e value and that from the Lagergren plot, which establish the first-order kinetics [46].

Pseudo-second-order kinetics is based on the adsorption capacity of solid phase. Furthermore, it is in agreement with chemisorption being the rate-controlling step and expressed as:

$$t/Q_t = 1/k_2 Q_e^2 + t/Q_e \quad (7)$$

where $k_2(\text{mg g}^{-1}\,\text{min}^{-1})$ is the pseudo-second-order rate constant of adsorption. The equilibrium adsorption capacity (Q_e) and k_2 can be found experimentally from the slope and intercept of plot t/Q_t versus t. The pseudo-second-order plot is linear $R^2 = 0.97$. However, the high difference between experimental and theoretical Q_e values lead to rejection of second-order kinetics (Fig. 8(b)) [47].

The possibility of intraparticle diffusion was explored using the intraparticle diffusion model. If the

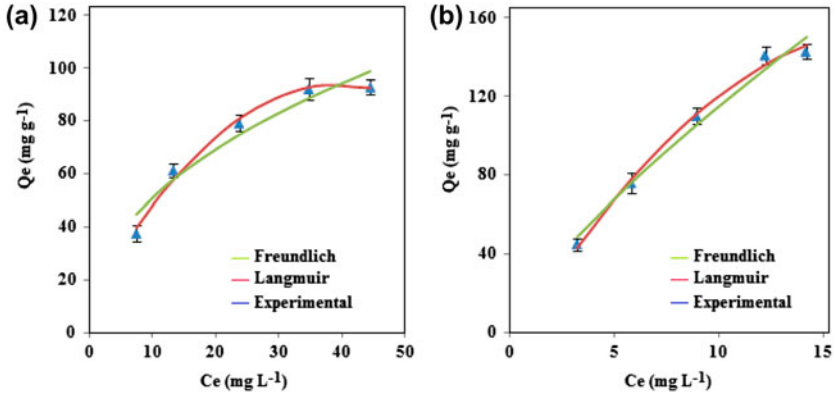

Fig. 7. The theoretical model fitted with experimental data using non-modified (a) and modified (b) magnetic perlite.

Table 2
Comparison of maximum monolayer adsorption of anionic dyes onto different adsorbents and equilibrium time

Adsorbent	Q_m	Equilibrium time (min)	References
CTAB-bentonite	109.89–133.33	40	[3]
Iron based waterworks sludge	5.44–833.34	100	[14]
$FeCl_2/FeCl_3$ PT nanoparticles	20	120	[41]
Orange peel	27.32–71.43	120	[44]
Pomegranate peel activated carbon	23.87–58.14	120	[46]
Ibuprofen modified MPT	416.66	1	This work

Table 3
kinetic parameters of adsorption of DR - 81 on to adsorbent

Analyte	Pseudo-first-order			Pseudo-second-order			Intraparticle diffusion		Film liquid diffusion
	Q_e	R^2	K_1	Q_e	R^2	K_2	K_p	R^2	R^2
DR-81	31.89	0.97	2.57	42.73	0.97	42.73	30.86	0.99	0.97

diffusion of ions on internal surfaces of pores and capillaries of the adsorbent is the rate-limiting step, the adsorption can be presented by the following equation:

$$Q_t = k_p t^{1/2} + C \tag{8}$$

where k_p represents intraparticle diffusion rate constant ($mg\,g^{-1}\,min^{-1/2}$) and C is a constant ($mg\,g^{-1}$ which gives information about the thickness of boundary layer. The plot of Q_t against $t^{1/2}$ yields a straight line passing through the origin in case of intraparticle diffusion (Fig. 8(c)) [48], the high linearity ($R^2 = 0.99$) of the intraparticle diffusion plot for the adsorption of DR-81 indicated that the intraparticle diffusion occurred. The line did not pass through an origin, thus it was not the only rate-limiting parameter.

The liquid film diffusion model, which explains the role of transport of the adsorbate from the liquid phase up to the solid phase boundary, can be expressed as:

$$\ln(1 - F) = -k_{fd}\, t \tag{9}$$

where F is the fractional attainment of equilibrium ($F = Q_t / Q_e$) and k_{fd} is the adsorption rate constant. The plot of $-\ln(1-F)$ versus t is illustrated in (Fig. 8(d)) [49].

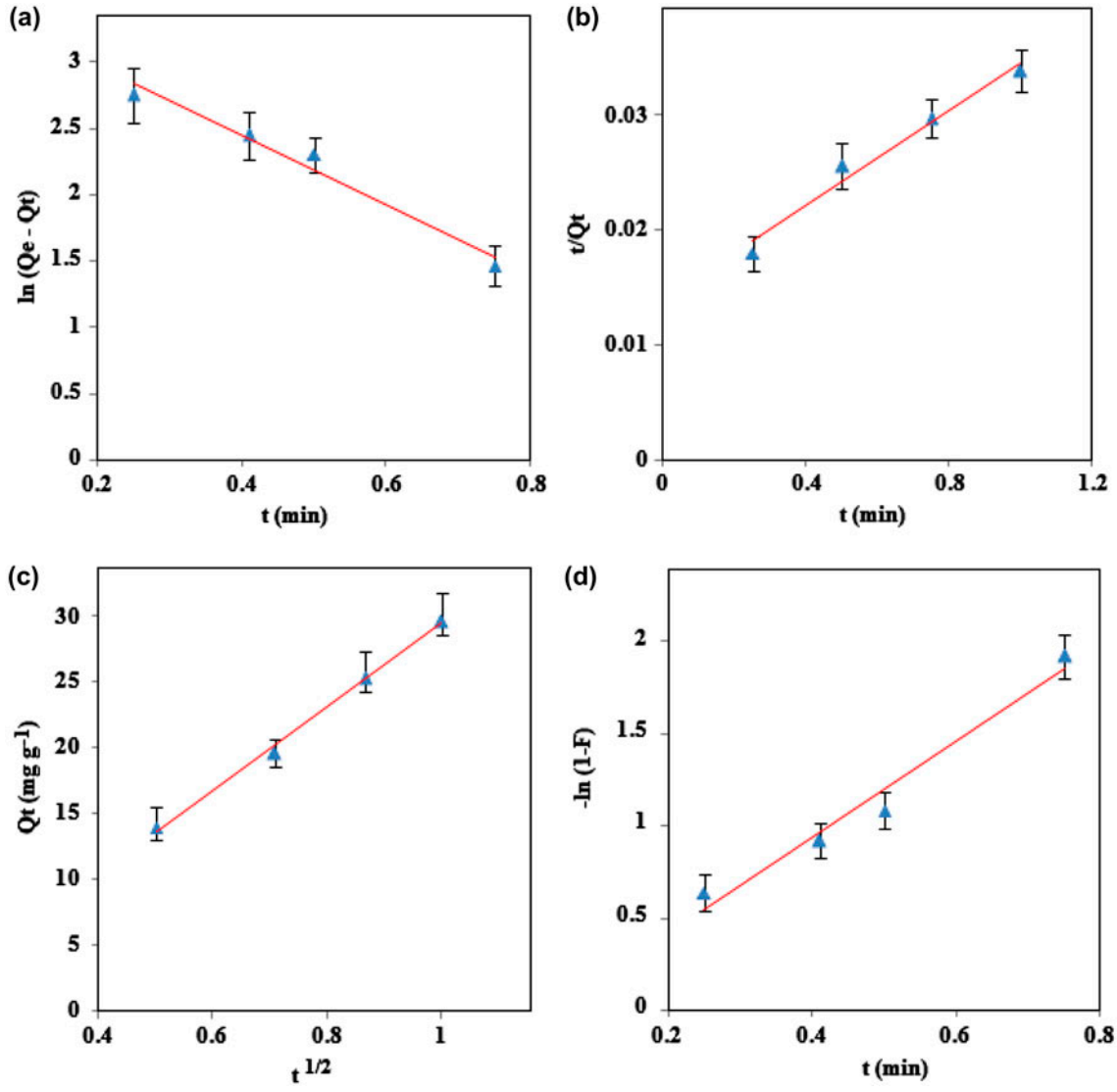

Fig. 8. First-order (a), second-order (b), intraparticle diffusion (c) and liquid film diffusion (d) models for adsorption of DR-81 onto modified MPT.
Note: (pH 4–6; dye concentration (C_0) = 20 mg L^{-1}; adsorbent dosage = 30 mg).

The possibility of film diffusion process was investigated by plotting −ln (1−*F*) versus *t*. As the curve for DR-81 exhibited linear plots with a correlation coefficient value of 0.97 and nonzero intercept (0.0751). This proved the role of film diffusion in the adsorption of DR-81, although the nonzero intercept limited applicability of this model.

3.7. Desorption and reusability

In order to find the best eluent, desorption experiments were performed under the optimized condition. According to effect of pH on dye removal, the adsorption was not feasible in alkaline solution. As a result, different solutions of NaOH (4.0×10^3, 2.0×10^4, 4.0×10^4, and 8.0×10^4 mg L^{-1}) were used for desorption process. The maximum desorption, however was up to 81%. The other candidate for this experiment; was organic reagents. Hence, various volumes of ethanol (2, 3, and 5 ml) were tested and better recovery results were obtained (52.24%, 86.12%, and 95.84%, respectively). Therefore, 5 ml of ethanol was selected as an effective eluent. The regeneration of the adsorbent is a key factor in improving process economics. Hence, modified sorbent, was subjected to several loadings with the sample solution and subsequent elution. The results show that, the removal efficiency remained

constant (90–95%) after four cycles of sorption and desorption.

3.8. Effect of competing ions

Wastewaters generally include various salts and metal ions which exert different effect on dye removal. Large amounts of salts cause high ionic strength. Moreover, they can compete with dyes which may significantly affect the dye adsorption performance of the adsorbent [50] Therefore, the effect of co-ions on the dye adsorption ability of prepared composite was evaluated by adding salts and metals individually to 50 mL solution containing 20 mg L^{-1} of DR-81. The method was applied under the optimized condition. Content of DR-81 in effluent was determined using UV–vis spectrophotometer and the removal efficiency was calculated. The results in Table 4 showed that the adsorption efficiency of the composite not significantly influenced by the presence of other ions. A small decrease was observed in adsorption yield with an increase in the concentration of competing ions. The maximum loss in the adsorption performance of the composite was about 10% under the experimental conditions studied. This may be due to the competition between dye and co-ions for the adsorptive sites on the adsorbent surface or change in the ionic strength of solution.

3.9. Analytical precision and detection limit

Under the optimum conditions, the relative standard deviation (RSD) of the method for DR-81 was 1.96%. It indicates that the method has good precision for the analysis of trace DR-81 from solution. The limit of detection was calculated by following equation:

$$D_L = 3S_B / m \quad (10)$$

where, S_B and m were standard deviation of the blank and the slope of the calibration graph. D_L value was found to be 0.02 ng/ml.

Table 4
Effect of interfering ions on % removal (DR-81 20 mg L^{-1}; sample volume 50 ml; sorbent 30 mg)

Ions	Ratio ion/DR-81	Removal%
Cl^-	2,000	90.62
SO_4^{2-}	4,000	92.84
PO_4^{3-}	2,000	96.01
K^+	2,200	90.67
Cu^{2+}	800	92.80
Na^+	2,000	90.61
Zn^{2+}	700	91.55
Ca^{2+}	1,000	93.04

4. Conclusions

In summary, MPT nanocomposite was prepared for the first time via an economic and green way using yellow pea powder as a reducing agent. Then it was modified with ibuprofen as a nontoxic reagent which enhanced the adsorption properties. The results of this study show that the prepared composite is a promising novel adsorbent, which was effectively used for the removal of anionic dyes such as DR-81. The adsorption process is so fast compared to other adsorption removal techniques, so much so that the equilibrium adsorption was achieved within 1 min. The effects of various operating conditions such as pH, adsorbent dosage, as well as initial dye concentration were studied and the optimum condition was obtained. Removal of DR-81 as an anionic dye was pH dependent and the maximum removal was attained at pH 4–6. The adsorption data were fitted well with Langmuir model. The maximum adsorption capacity based on the Langmuir model after the modification was enhanced from 142.85 to 416.66 mg $L^{-1}$for DR-81. Desorption of the dye carried out using 5 ml ethanol. Thus, the ibuprofen modified magnetic perlite found to be an effective, low-cost adsorbent and also the presented eco-friendly method of MNP synthesis could be an alternative to the other synthesis routs in order to make a dye removal, green and effective.

Acknowledgment

Support for this investigation by the Research Council of the University of Tehran through grants is gratefully acknowledged.

References

[1] G. Moussavi, R. Khosravi, The removal of cationic dyes from aqueous solutions by adsorption onto pistachio hull waste, Chem. Eng. Res. Des. 89 (2011) 2182–2189.
[2] R. Akkaya, B. Akkaya, Adsorption isotherms, kinetics, thermodynamics and desorption studies for uranium and thorium inos from aqueous solution by novel microporous composite P(HEMA-EP), J. Nucl. Mater. 434 (2013) 328–333.
[3] B. Zohra, K. Aicha, S. Fatima, B. Nourredine, D. Zoubir, Adsorption of Direct Red 2 on bentonite modified by cetyltrimethylammonium bromide, J. Chem. Eng. 136 (2008) 295–305.

[4] P.C.C. Faria, J.J.M. Órfão, M.F.R. Pereira, Adsorption of anionic and cationic dyes on activated carbons with different surface chemistries, Water Res. 38 (2004) 2043–2052.
[5] M.T. Sulak, H.C. Yatmaz, Removal of textile dyes from aqueous solutions with eco-friendly biosorbent, Desalin. Water Treat. 37 (2012) 169–177.
[6] W.S. Wan Ngah, L.C. Teong, M.A.K.M. Hanafiah, Adsorption of dyes and heavy metal ions by chitosan composites, Carbohydr. Polym. 83 (2011) 1446–1456.
[7] J. Wolska, M. Bryjak, Preparation of polymeric microspheres for removal of boron by means of sorption-membrane filtration hybrid, Desalination 283 (2011) 193–197.
[8] B. An, Q. Liang, D. Zhao, Removal of arsenic (V) from spent ion exchange brine using a new class of starch-bridged magnetite nano particles, Water Res. 45 (2011) 1961–1972.
[9] A. Afkhami, M.S. Tehrani, H. Bagheri, Modified-maghemite nanoparticles as an efficient adsorbent for removing some cationic dyes from aqueous solution, Desalination 263 (2010) 240–248.
[10] V.S. Mane, P.V. Vijay Babu, Studies on the adsorption of Brilliant Green dye from aqueous solution onto low cost NaOH treated sawdust, Desalination 273 (2011) 321–329.
[11] T. Nishimiura, Y. Umetsu, Oxidative precipitation of arsenic (III) with manganese(II) and iron (II) in dilute acidic solution by ozone, Hydrometallurgy 62 (2001) 83–92.
[12] A.l. del Rio, J. Fernández, J. Molina, J. Bonastre, F. Cases, Electrochemical treatment of a synthetic wastewater contining a sulphonated azo dye. Determination of naphthalenesulphonic compounds produced as main by-product, Desalination 273 (2011) 428-435.
[13] N.A. Oladoja, I.A. Olodala, O.A. Alimi, T.A. Akinnifesi, G.A. Olaremu, Iron incorporated rice husk silica as an adsorbent for hexavalent chromium attenuation in aqueous system, Chem. Eng. Res. Des. 91 (2013) 2691–2702.
[14] B. Kayranli, Adsorption of textile dyes onto iron based wasteworks sludge from aqueous solution; isotherm, kinetic and thermodynamic study, Chem. Eng. J. 173 (2011) 782–791.
[15] F. Doulati Ardejani, K. Badii, N.Y. Limaee, S.Z. Shafaei, A.R. Mirhabibi, Adsorption of Direct Red 80 dye from aqueous solution onto almond shell: Effect of pH, initial concentration and shell type, J. Hazard. Mater. 151 (2008) 730–737.
[16] G. Crini, Non-conventional low-cost adsorbents for dye removal: A review, Bioresour. Technol. 97 (2006) 1061–1085.
[17] M.C. Shih, Kinetics of the batch adsorption of methylene blue from aqueous solutions onto rice husk: Effect of acidmodified process and dye concentration, Desalin. Water Treat. 37 (2012) 200–214.
[18] Y. Safa, H.N. Bhatti, Bioadsorption of Direct Red-31 and Direct orange-26 dyes by rice husk: Application of factorial design analysis, Chem. Eng. Res. Des. 89 (2011) 2566–2574.
[19] E. Forgacs, T. Cserhati, G. Oros, Removal of synthetic dyes from wastewaters, Environ. Int. 30 (2004) 953–971.
[20] N. Tekin, A. Dinçer, Ö. Demirbaş, M. Alkan, Adsorption of cationic polyacrylamide (C-PAM) on expanded perlite, Appl. Clay Sci. 50 (2010) 125–129.
[21] M.G. Mostafa, Y. Chen, J. Jean, C. Liu, Y. Lee, Kinetics and mechanism of arsenate removal by nanosized iron oxid-coated perlite, J. Hazard. Mater. 187 (2011) 89–95.
[22] D.N. Thanh, M. Singh, P. Ulbrich, N. Strnadova, F. Štěpánek, Perlite incorporating Υ-Fe_2O_3 and α-MnO_2 nanomaterials: Preparation and evaluation of a new adsorbent for As (V) removal, Sep. Purif. Technol. 82 (2011) 93–101.
[23] M. Torab-Mostaedi, A. Ghaemi, H. Ghassabzadeh, M. Ghannadi-Maragheh, Removal of strontium and barium from aqueous solutions by adsorption onto expanded perlite, Can. J. Chem. Eng. 89 (2011) 1247–1254.
[24] O. Demirba, M. Alkan, M. Doğan, The removal of victroia blue from aqueous solution by adsorption on low-cost material, Adsorption 8 (2002) 341–349.
[25] M. Dogan, M. Alkan, Removal of methyl violet from aqueous solution by perlite, J. Colloid Interface Sci. 267 (2003) 32–41.
[26] G. Vijayakumar, M. Dharmendirakumar, S. Renganathan, S. Sivanesan, G. Baskar, K.P. Elango, Removal of Congo Red from aqueous solutions by perlite, Clean 37 (2009) 355–364.
[27] M. Dogan, M. Alkan, A. Türkyilmaz, Y. Özdemir, Kinetics and mechanism of removal of methylene blue by adsorption onto perlite, J. Hazard. Mater. B109 (2004) 141–148.
[28] H.Y. Zhu, F.U. Yq, R. Jiang, J.H. Jiang, L. Xiao, G.M. Zeng, S.L. Zhao, V.Y. Wang, Adsorption removal of congo red onto magnetic cellulose/Fe_3O_4/activated carbon composite: Equilibrium, kinetic and thermodynamic studies, Chem. Eng. J. 173 (2011) 494–502.
[29] H.Y. Zhu, R. Jiang, L. Xiano, W. Li, A novel magnetically separable Υ-Fe_2O_3/ crosslinked chitosan adsorbent: Preparation, characterization and adsorption application for removal of hazardous azo dye, J. Hazard. Mater. 179 (2010) 251–257.
[30] G. Zhang, J. Qu, H. Liu, A.T. Cooper, R. Wu, $CuFe_2O_4$/activated carbon composite: A novel magnetic adsorbent for the removal of acid orange II, Chemosphere 68 (2007) 1058–1066.
[31] S.K. Giri, N.N. Das, G.C. Pradhan, Synthesis and characterization of magnetic nanoparticles using waste iron ore tailings for adsorptive removal of dyes from aqueous solution, Colloids Surf. A 389 (2011) 43–49.
[32] S. Venkateswarlu, Y.S. Rao, T. Balaji, B. Prathima, N.V.V. Jyothi, Biogenic synthesis of Fe_3O_4 magnetic nanoparticles using plantain peel extract, Mater. Lett. 100 (2013) 241–244.
[33] W. Lu, Y. Shen, A. Xie, W. Zhang, Green synthesis and characterization of superparamagnetic Fe_3O_4 nanoparticles, J. Magn. Magn. Mater. 322 (2010) 1828–1828.
[34] A.K. Mittal, Y. Chisti, U.C. Banerjee, Synthesis of metallic nanoparticles using plant extracts, Biotechnol. Adv. 31 (2013) 346–356.
[35] K.B. Narayanan, N. Sakthivel, Green synthesis of biogenic metal nanoparticles by terrestrial and aquatic phototrophic and heterotrophic eukaryotes and biocompatible agents, Adv. Colloid Interface Sci. 169 (2011) 59–79.

[36] Y. Cai, Y. Shen, A. Xie, S. Li, X. Wang, Green synthesis of soya bean sprouts-mediated superparamagnetic Fe_3O_4 nanoparticles, J. Magn. Magn. Mater. 322 (2010) 2938–2943.
[37] O.V. Kharissova, H.V.R. Dias, B.I. Kharisov, B.O. Pérez, V.M.J. Pérez, The greener synthesis of nanoparticles, Trends Biotechnol. 31 (2013) 240–248.
[38] A. Demir, R. Topkaya, A. Baykal, Green synthesis of superparamagnetic Fe_3O_4 nanoparticles with maltose: Its magnetic investigation, Polyhedron 65 (2013) 282–287.
[39] M. Mahdavi, F. Namvar, M.B. Ahma, R. Mohamad, Green biosynthesis and characterization of magnetic iron oxide (Fe_3O_4) nanoparticles using seaweed (*Sargassum muticum*) aqueous extract, Molecules 18 (2013) 5954–5964.
[40] T. Wang, X. Jin, Z. Chen, M. Megharaji, R. Naidu, Green synthesis of Fe nanoparticles using eucalyptus leaf extracts for treatment of eutrophic wastewater, Sci. Total Environ. 466–467 (2014) 210–213.
[41] M.R. Heydartaemeh, F. Doulati Ardejani, K. Badii, K. Seifpanahi Shabani, S.E. Mousavi, FeCl2/FeCl3 perlite nanoparticles as a novel magnetic material for adsorption of green malachite dye, Arab. J. Sci. Eng. 39 (2014) 3383–3392.
[42] S. Zodi, B. Merzouk, O. Potier, F. Lapicque, J. Leclerc, Direct Red 81 dye removal by a continuous flow electrocoagulation/flotation reactor, Sep. Purif. Technol. 108 (2013) 215–222.
[43] A. Mittal, J. Mittal, A. Malviya, V.K. Gupta, Adsorptive removal of hazardous anionic dye "Congo Red" from wastewater using waste materials and recovery by adsorption, J. Colloid Interface Sci. 340 (2009) 16–26.
[44] A. Khaled, A. El-Nemr, A. El-Sikaily, O. Abdelwahab, Treatment of artificial textile dye effluent containing Direct Yellow 12 by orange peel carbon, Desalination 238 (2009) 210–232.
[45] Y.S. Ho, Selection of optimum sorption isotherm, Carbon 42 (2004) 2113–2130.
[46] N.K. Amin, Removal of Direct Blue-106 dye from pomegranate peel: Adsorption equilibrium and kinetics, J. Hazard. Mater. 165 (2009) 52–62.
[47] H. Yang, B. Sun, H. Wang, Removal of anionic dye from aqueous solution by magnesium silicate gel, Desalin. Water Treat. 52 (2014) 7685–7692.
[48] M.M. Abd El-Latif, A.M. Ibrahim, Adsorption, kinetic and equilibrium studies on removal of basic dye from aqueous solutions using hydrolyzed Oak sawdust, Desalin. Water Treat. 6 (2009) 252–268.
[49] A. Chatterjee, S. Schiewr, Multi-resistance kinetic models for biosorption of Cd by raw and immobilized citrus peels in batch and packed-bed columns, Chem. Eng. J. 244 (2014) 105–116.
[50] S.T. Akar, T. Alp, D. Yilmazer, Enhanced adsorption of Acid Red 88 by an excellent adsorbent prepared from alunite, J. Chem. Technol. Biotechnol. 88 (2013) 293–304.